Applied Physics Letters ARTICLE scitation.org/journal/apl

Shockwave generation by electrical explosion of cylindrical wire arrays in hydrogen peroxide/water solutions

Cite as: Appl. Phys. Lett. **116**, 243702 (2020); doi: 10.1063/5.0011226
Submitted: 20 April 2020 · Accepted: 3 June 2020 ·
Published Online: 16 June 2020

View Online Export Citation CrossMark

A. Rososhek,[a] S. Efimov, D. Maler, A. Virozub, and Ya. E. Krasik

AFFILIATIONS

Physics Department, Technion, Haifa 3200003, Israel

[a]Author to whom correspondence should be addressed: sasharos@campus.technion.ac.il

ABSTRACT

We report the results of experiments investigating the implosion of a shock generated by the electrical explosion of a cylindrical aluminum wire array immersed in a >80% hydrogen peroxide/water solution. This solution was chosen as an additional energy source to the supplied electrical energy to generate the imploding flow with higher velocity. The experiments were conducted using a generator with the stored energy of ∼4.8 kJ, delivering to the array a ≤280 kA current rising during ∼1 μs. The backlighted images of the imploding shocks were recorded using a streak camera. Using different diameter wires, the explosion of arrays, characterized by critically damped and underdamped discharges, was studied. The experiments revealed that an array explosion in a 92% H_2O_2/H_2O solution results in the second strong shock generated after the peak of the deposited electrical power, a solid indication of H_2O_2 detonation. This second shock converges ∼40% faster than the first strong shock generated by the wire explosion. One-dimensional hydrodynamic simulations of the shock convergence in H_2O_2/H_2O solutions support this proposition.

Published under license by AIP Publishing. https://doi.org/10.1063/5.0011226

Recent developments in the study of underwater electrical explosions of cylindrical or quasi-spherical wire arrays[1–3] accompanied by the generation of strong converging shocks show that this approach allows one to obtain pressures $>10^{11}$ Pa in the vicinity of the implosion axis or origin. However, the results obtained[4] also show that the shock velocity increases only at radii $r \leq 0.5$ mm while it remains almost constant along the main convergence path. Therefore, it is important to find an additional energy source to accelerate the shock during its main convergence path to achieve even larger thermodynamic parameters of the matter in the implosion vicinity. A shock-ignited medium can be considered as a powerful energy source when a detonation[5] process delivers energy to the flow generating a strong shock. Earlier studies[6] show that a H_2O_2/H_2O solution at room temperature with H_2O_2 concentration $\eta > 85\%$ is shock detonatable. It was shown that detonation ignition depends on the pressure behind the planar shock front, and the detonation wave velocity depends on the value of η. Also, both numerical simulations[7] and experimental data[8] suggest that detonation ignition occurs behind the shock front when the pressure is above 10 GPa. However, there is no data on H_2O_2/H_2O solution detonation at higher than room temperatures, as well as by converging cylindrical shock.

In the present research, we study converging shocks generated by an electrical explosion of cylindrical Al wire arrays, immersed in H_2O_2/H_2O solutions of various concentrations of H_2O_2. Since the pressure and temperature, necessary for H_2O_2/H_2O solution detonation, are uncertain parameters, we carried out experiments with almost critically damped (*aperiodic*) and underdamped fast decaying (*periodic*) discharges. An aperiodic discharge generates the fastest shock[9] when the major part of the stored energy is deposited into the wires during less than a quarter-period of the underdamped discharge. A periodic discharge is characterized by a weaker shock generation, but the discharge channel reaches a higher temperature during the current restrike.

The direct measurement of thermodynamic parameters of liquid in the vicinity of the implosion axis is challenging because ns-time and μm-space resolution are required. Therefore, these parameters are estimated employing one-dimensional hydrodynamic (1DHD) modeling[4] coupled with the equation of state (EOS) for the liquid and the wire material.[10] Because of the absence of EOS for H_2O_2/H_2O solutions, for 1DHD simulations, a polytropic EOS[11] for water was rescaled with H_2O_2 densities.[7] The 1DHD simulation requires as input the time-dependent energy density deposition calculated using the measured

Published under license by AIP Publishing

resistive voltage and current waveforms. The simulation output is verified by comparing the measured shock time-of-flight (TOF) with the calculated result and by validating that the energy transfer efficiency to the converging water flow does not exceed ~12%.[3]

Experiments were conducted using a μs-timescale generator[12] with the stored energy of ~4.8 kJ at a charging voltage of 31 kV. The generator produced a ~380 kA-amplitude current pulse with a rise time of ~1.2 μs when an inductive load of ~17 nH was used. Electrical explosions of 45 mm long, 5, 10, and 20 mm diameter Cu or Al wire arrays consisting of 40 wires were studied. For explosions in the H_2O_2/H_2O solution, the array was placed inside a hermetically closed dielectric box (total volume of ~17 cm^3) filled with the solution, which was immersed in the water-filled chamber. Since the H_2O_2/H_2O solution causes intense oxidation of Cu, only Al wires were used in these experiments. Cu and Al wire array explosions in deionized water were performed as reference for the Al wire array explosion experiments in H_2O_2/H_2O solutions. The diameter of the wires was varied from 50 μm to 127 μm for Al and from 80 μm to 114 μm for Cu wires to obtain similar types of discharge. Below we shall use the term "Al 40×D μm d mm" to refer in shorthand to an explosion of 40 D μm diameter Al wires making up a cylindrical array of diameter d mm. The term 80% solution is used to refer to the H_2O_2 concentration in water.

The experimental setup is shown in Fig. 1. A continuous-wave laser (single-mode, 532 nm, 1.5 W) was used for the backlighted streak image of the shock using an Optoscope SC-10 camera (Optronis GmbH). The discharge current and voltage drop across an array were measured by a Rogowski coil and a Tektronix voltage divider, respectively. To obtain reproducible waveforms and shadow images, at least two shots of the generator were carried out for each experimental configuration (except explosions in 92% solutions, for which the destruction of the setup was excessive). To synchronize the generator and the streak camera, a DG645 pulse delay unit and a light-emitting diode (LED) producing a marker on the streak image were used. The timing of the marker and the peak of the calculated electrical power were used to compute the shock's TOF. The timing of the light resulting from the shock implosion[12] and recorded on the streak image was verified to an accuracy of ≤30 ns using a Hamamatsu R7400U-04 photomultiplier tube.

The main parameters of wire array explosions are listed in Table I. Note that the current and voltage waveforms for explosions in

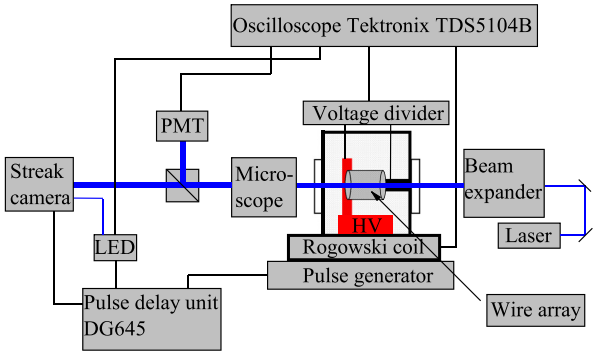

FIG. 1. Experimental setup.

H_2O_2 solutions, and different array diameters, but with the same number and diameter of wires were quantitatively similar to those seen in water. Contrary to the periodic discharges (Al 40 × 75 μm 5 mm in Table I), the aperiodic ones (Al 40 × 127 μm 10 mm in Table I) are characterized by larger energy deposition (>800 J) prior to the appearance of the peak power. For Al 40 × 127 μm 10 mm, the single wire resistance reaches ~10 Ω at peak power, indicating the formation of low temperature and density plasma, whereas for Al 40 × 75 μm 5 mm, it reaches ~20 Ω and drops to ~4 Ω with a current restrike, indicating the formation of a higher temperature and density plasma. These discharges, characterized by different temperatures of the plasma channels and parameters of the generated shocks, were used to study the detonation in the H_2O_2 solution.

Let us note that the same shock TOF was obtained for underwater aperiodic explosions of Cu and Al arrays with either 10 mm or 20 mm diameter with a similar peak deposited power of ~12 GW. No differences in the TOF data were obtained for the periodic underwater explosions of these arrays, indicating no measurable effect of Al combustion on the shock convergence for wire array diameters ≤20 mm. For 5 mm-diameter arrays and aperiodic explosions, the weak shock (~1650 m/s) is formed by the wire's phase transition[13] ~500 ns earlier than the peak of deposited power. This weak shock reaches the axis prior to the arrival of the strong shock generated close to the peak of the power. As a result, the strong shock trajectory is smeared by the slightly compressed water flow behind the weak shock front.

In Figs. 2(a) and 2(b), we present typical streak images of the shocks superimposed by the time dependence of the power deposited into the Al wire arrays during aperiodic explosions in 92% solution and water. The measured strong shock TOFs for these explosions were 1450 ± 30 ns [Fig. 2(a)] and 1640 ± 30 ns [Fig. 2(b)]. In Fig. 2, we also point out the LED marker, the weak/strong shocks, and the overtake (the point in time when the strong shock overtakes the weak shock). These overtakes occur at $t \approx 1450$ ns and $t \approx 1900$ ns for explosions in 92% solution and water, respectively. The calculated velocities of weak and strong shocks in 92% solution and water are ~1800 m/s/–2600 m/s and ~1650 m/s/–2700 m/s, respectively. In Fig. 2(a) there is an additional feature at $t \approx 1850$ ns, corresponding to the second inflection of the shock's trajectory indicating that another, stronger (second) shock is overtaking the rest. This will be addressed below.

Furthermore, in Fig. 2 a difference in the light emission is seen in the vicinity of the implosion ($r \approx 0.1$ mm). For the explosion in 92% solution, a radially nonuniform narrow light splash before the shock [see Fig. 2(a)] spreads along the shock trajectory starting at $r \approx 1$ mm. A similar light emission, but less intense, was seen in explosions in the 80% solution. This light emission cannot be related to thermal emission from the compressed liquid behind the shock front. At this radial distance, the compression is $\delta = \rho/\rho_0 \leq 1.5$, where ρ and ρ_0 are the shock-compressed H_2O_2/H_2O solution and normal densities, respectively. This compression corresponds (in the case of water) to a temperature less than 500 °C. Thus, the most likely reason for this light emission is the detonation of the H_2O_2 solution. In contrast to the H_2O_2 solution, explosions in water produce only a small-size radially uniform light blob (~60 μm diameter) and ~50 ns prior to the observable implosion [see Fig. 2(b)]. This is similar to the result of research,[12] where a short-duration light emission in the vicinity of the shock implosion was obtained in cylindrical wire array explosions in water.

Published under license by AIP Publishing

TABLE I. Main parameters of wire array explosions.

Wire material/ diameter (μm)	Medium	Rise time[a] (ns)	Explosion time[a] (ns)	First current maximum[b] (kA)	Second current maximum[b] (kA)	Voltage amplitude[b] (kV)	Power (GW)	Energy deposited until maximum power (kJ)	Energy deposited until the first zero in the current (kJ)
Al 40 × 75μm 5 mm	Water	410	470	150	125	54	6.6	0.5	4.7
Al 40 × 75μm 5 mm	92% H_2O_2	400	460	145	140	55	6.4	0.5	4.5
Al 40 × 127 μm 10 mm	Water	830	1000	250	none	58	12.2	1.6	4.4
Al 40 × 127 μm 10 mm	92% H_2O_2	830	950	260	none	55	12.8	1.4	4.5

[a]The error in the rise time and explosion time is ∼2.5%.
[b]The errors in the electrical measurements are ∼5% and ∼10% for the voltage and current, respectively.

In addition to the differences seen in the TOF and the light emission from before/behind the shock front in 92% solution and water, a large difference in the destruction of the experimental setup was also observed. For the explosion in water, only the dielectric supports of the wire electrode holder were damaged. However, each explosion in 92% solution resulted in the complete destruction of the 15 mm thick perspex windows (see Fig. 1). Four M6 bolts, holding the Al flange (80 × 55 × 10 mm: length × width × height) used to support optical windows, were ejected to a few meters away, and the flange was bent ∼5 mm outwards. Based on the material data of Al[14] and perspex window[15] and assuming elastic deformations only, we estimate,[16] as a lower bound, that at least ∼1 kJ energy is required to cause such deformation. These damages strongly indicate the existence of a powerful additional source like the detonation of the H_2O_2 solution.

In Fig. 3, we present the time evolution of shock velocities calculated using the streak images data (Fig. 2) and results of 1DHD simulations for the aperiodic explosion of Al 40 × 127 μm 10 mm array in 92% solution and water. For both media, the weak shock is overtaken by the strong shock (see jumps in shock velocities). However, the second jump [see the second inflection point, magnified in Fig. 2(a)] seen at $t \approx 1830$ ns (blue curve in Fig. 3), in the H_2O_2 solution indicates the overtake of the first shock generated prior to peak power deposited into the wires by a stronger second shock generated later in time. Although the evolution of this second strong shock prior to the jump to $v \approx 3800$ m/s is not seen, it is likely to arise due to H_2O_2 detonation in the vicinity of the exploding wires. Furthermore, Figs. 2 and 3 show that the explosion in 92% solution results in faster overtake and smaller (∼200 ns) TOF, than for explosions in water. These data also suggest a larger energy deposition into the H_2O_2 solution flow.

The simulated shock velocity in 92% solution (Fig. 3) does not agree with the experimental results, in contrast to the water, for which both the shock TOF and the velocity are consistent with the experiment. To obtain the second velocity jump in simulations, an additional energy source had to be added at least 200 ns after the peak in the power. For example, a ∼4 kJ, 50 ns Full-Width at Half Maximum Gaussian-like energy source artificially introduced in the vicinity of the exploding wires result in a second velocity jump obtained in the experiment. Finally, in the vicinity of the implosion, the shock velocity obtained in 92% solution exceeds ∼4500 m/s that corresponds to a pressure of $\sim 10^{10}$ Pa and ∼1600 m/s flow velocity behind the shock front.[7]

Next, we consider the results with periodic discharges when the explosion of the Al wire array occurs earlier than for an aperiodic discharge (see Table I). This leads to a smaller time difference between the generation of the weak and strong shocks resulting in the overtake of the weak shock by the strong one even for 5 mm diameter arrays. In Fig. 4, the streak images of the shocks generated by exploding Al 40 × 75 μm 5 mm wire arrays in 92% solution and water are shown. One can see features similar to those seen in Fig. 2. For instance, in Fig. 4(a) the weak shock of velocity $v \approx 1800$ m/s (∼5% above the sound velocity in 92% solution[7]) is overtaken by the strong shock propagating with $v \approx 2500$ m/s at $t \approx 900$ ns relative to the discharge current beginning. Additionally, in Fig. 4(a) there is second strong shock propagating toward the axis. Although the trajectory of this shock is slightly smeared by the compressed liquid, its, almost

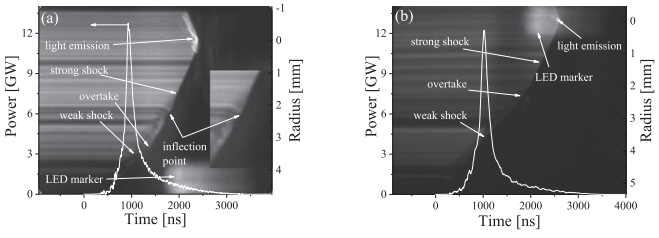

FIG. 2. Backlighted streak images of the converging shocks generated by an Al 40 × 127 μm 10 mm wire array explosion in 92% solution (a) and in water (b).

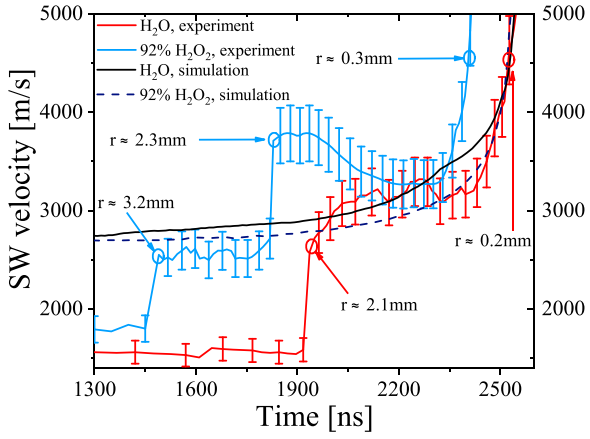

FIG. 3. Shock velocities calculated from the streak images in Fig. 2 and 1DHD simulated values. Initial time (1300 ns) corresponds to $r \approx 3.5$ mm (cyan) and $r \approx 3.2$ mm (red).

Published under license by AIP Publishing

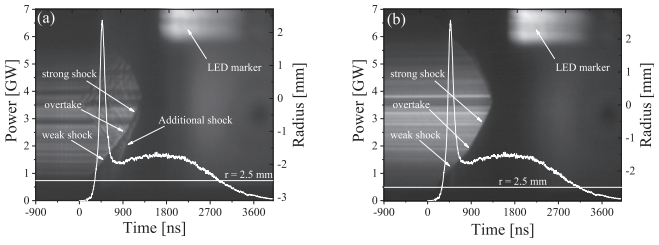

FIG. 4. Backlighted streak images of the converging shocks generated by Al 40 × 75 μm 5 mm wire array explosions in 92% solution (a) and water (b) superimposed by the deposited power's time dependence.

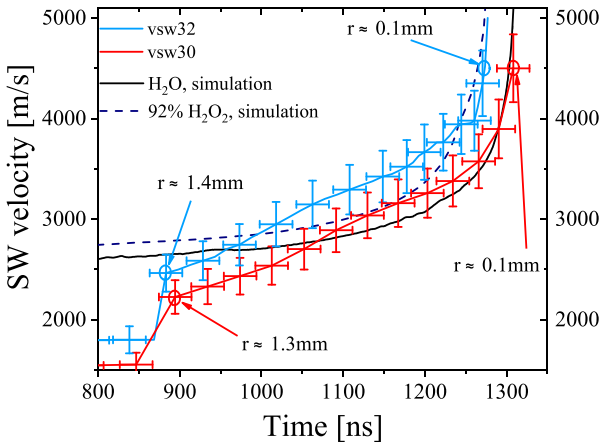

FIG. 5. Shock velocities calculated from the streak images in Fig. 4 and 1DHD simulated shock velocities. Initial time (800 ns) corresponds to $r \approx 1.5$ mm (cyan) and $r \approx 1.4$ mm (red).

constant, velocity can be estimated to be $v \approx 3500$ m/s. The TOF analysis showed that the generation of this shock occurs with a ~250 ns delay relative to the maximum of the deposited power. Thus, one can suppose that the detonation of the 92% solution, when current restrike occurs and intense Al combustion begins,[17] leads to the formation of this shock due to increased temperature at the discharge channel/solution interface.

In Fig. 5 we show the time evolution of shock velocities [not including the additional shock seen in Fig. 4(a)] calculated using the streak images data (Fig. 4) and the results of 1DHD simulations for the periodic explosion of Al 40 × 75 μm 5 mm array in 92% solution and water. Note that the jumps in velocities due to the overtake of the weak shock by the strong one are almost the same for explosions in 92% solution and in water. This indicates that the shock generation process in both media is similar, that is, the H_2O_2 solution does not detonate at the time when the strong shock is generated. One can also see that in the vicinity ($r < 0.5$ mm) of the implosion, there is a satisfactory agreement between the measured velocities in 92% solution and in water with the results of 1DHD simulations.

To summarize, results of Al wire arrays explosion experiments in high concentration H_2O_2 solutions strongly indicate that hydrogen peroxide detonates and delivers additional energy to the converging flow allowing to achieve considerably higher pressures and temperatures of the liquid in the vicinity of the implosion.

We thank Dr. A. Kuznetsov for his technical assistance in preparing the H_2O_2 solutions. We are grateful to Dr. J. Leopold, Dr. V. Gurovich, and Dr. S. Chefranov for fruitful discussions and S. Gleizer for generous technical assistance. This research was supported by the Israeli Science Foundation Grant No. 492/18 and in part by the Center for Absorption in Science, Ministry of Immigrant Absorption, State of Israel.

DATA AVAILABILITY

The data that support the findings of this study are available from the corresponding author upon reasonable request.

REFERENCES

[1]S. N. Bland, Y. E. Krasik, D. Yanuka, R. Gardner, J. MacDonald, A. Virozub, S. Efimov, S. Gleizer, and N. Chaturvedi, Phys. Plasmas **24**, 082702 (2017).
[2]O. Antonov, S. Efimov, D. Yanuka, M. Kozlov, V. T. Gurovich, and Y. E. Krasik, Appl. Phys. Lett. **102**, 124104 (2013).
[3]Y. E. Krasik, S. Efimov, D. Sheftman, A. Fedotov-Gefen, O. Antonov, D. Shafer, D. Yanuka, M. Nitishinskiy, M. Kozlov, L. Gilburd, G. Toker, S. Gleizer, E. Zvulun, V. Tz. Gurovich, D. Varentsov, and M. Rodionova, IEEE Trans. Plasma Sci. **44**, 412 (2016); and references therein.
[4]G. Bazalitski, V. T. Gurovich, A. Fedotov-Gefen, S. Efimov, and Y. E. Krasik, Shock Waves **21**, 321 (2011).
[5]A. S. Kompaneets, *Shock Waves* (Physmathgiz, Moscow, 1963) (in Russian).
[6]R. Engelke, S. A. Sheffield, and L. L. Davis, J. Phys. Chem. A **104**, 6894–6898 (2000).
[7]M. R. Armstrong, J. M. Zaug, N. Goldman, I. F. W. Kuo, J. C. Crowhurst, W. M. Howard, J. A. Carter, M. Kashgarian, J. M. Chesser, T. W. Barbee, and S. Bastea, J. Phys. Chem. A **117**, 13051 (2013).
[8]L. L. Gibson, B. Bartram, D. M. Dattelbaum, S. A. Sheffield, and D. B. Stahl, AIP Conf. Proc. **1195**, 133 (2009).
[9]A. Rososhek, S. Efimov, A. Virozub, D. Maler, and Y. E. Krasik, Appl. Phys. Lett. **115**, 074101 (2019).
[10]S. P. Lyon and J. D. Johnson, "SESAME: The Los Alamos National Laboratory equation-of-state database," Report No. LA-UR-92–3407 (Los Alamos National Laboratory, 1992).
[11]Y. B. Zeldovich and Y. P. Raizer, *Physics of Shock Waves and High-Temperature Hydrodynamic Phenomena*, 2nd ed. (Academic Press, New York/London, 1966).
[12]S. Efimov, A. Fedotov, S. Gleizer, V. T. Gurovich, G. Bazalitski, and Y. E. Krasik, Phys. Plasma **15**, 112703 (2008).
[13]A. Rososhek, S. Efimov, S. V. Tewari, D. Yanuka, and Y. E. Krasik, Phys. Plasmas **25**, 102709 (2018).
[14]C. Comte and J. von Stebut, Surf. Coat. Technol. **154**, 42–48 (2002).
[15]C. Ishiyama and Y. Higo, J. Polym. Sci., Part B **40**, 460 (2002).
[16]L. D. Landau and E. M. Lifshitz, *Theory of Elasticity* (Pergamon Press, 1986).
[17]A. Rososhek, S. Efimov, A. Goldman, S. V. Tewari, and Y. E. Krasik, Phys. Plasmas **26**, 053510 (2019).

Published under license by AIP Publishing